A subset of oligodendrocytes generated from radial glia in the dorsal spinal cord

Matthew Fogarty, William D Richardson and Nicoletta Kessaris

The Wolfson Institute for Biomedical Research and Department of Biology, University College London (UCL), Gower Street, London WC1E 6BT, UK.

***Correspondence**:* Bill Richardson, tel +44 (0)20 7679 6729 w.richardson@ucl.ac.uk

Keywords: Dbx, Cre, spinal cord, radial glia, neurons, astrocytes, oligodendrocytes.

Running title: Dorsally-derived oligodendrocytes

Abstract (149 words)

Many oligodendrocytes in the spinal cord are

data from chick-quail chimeras that raise the possibility of dorsal as well as ventral sources of OLPs in birds (Cameron-Curry and Le-Douarin, 1995; Pringle et al., 1998; Richardson et al., 1997).

In the present study we used Cre-mediated recombination in transgenic mice to follow the

described (Lee et al., 2001), thereby removing the entire coding region of Dbx1 and replacing it with iCre.

The modified PAC DNA was linearized by *Asc*I digestion. PFGE was used to purify the PAC insert away from small vector fragments. This linear PAC DNA was concentrated into a 4% low melting point agarose gel. Following β-agarase (New England Biolabs) digestion and

1:8000 (a gift from T. Jessell); monoclonal CC1 at 1:400 (Merck Biosciences); guinea pig anti-Lbx1 at 1:8000 (gift from T. Jessell); monoclonal anti-Lim2 at 1:5 (DSHB); monoclonal anti-Lim3 at 1:20 (DSHB) and monoclonal anti-S100β at 1:400 (Sigma). Primary antibodies were applied overnight at 4°C. Secondary antibodies were rhodamine- , AMCA- or fluorescein- conjugated anti-rabbit, -goat, -rat, -guinea pig or -mouse IgM or anti-mouse IgG at 1:200 (Pierce) and were applied for 60 minutes at room temperature. To allow Olig2 and GFP double labelling, a goat anti-rabbit IgG Fab fragment (Jackson) was used to effectively convert rabbit Olig2 into a goat antibody, prior to detection with an anti-goat IgG secondary antibody. All antibodies were diluted in PBS containing 10% serum and 0.1% (v/v) Triton X-100. Following antibody treatment, sections were stained with Hoescht (Sigma) and post-fixed for 5 minutes in 4% PFA. Sections were mounted under coverslips in Citifluor anti-fade reagent (City University, UK).

Spinal cord cultures

Spinal cord cultures were done as previously described (Kessaris et al, 2004). Briefly, spinal cords from E12.5 mouse embryos were dissected away from surrounding tissue in Hepes-buffered minimal essential medium (MEM-H) (Invitrogen) and dissociated by incubation in 0.0125% (w/v) trypsin in Earle's balanced salt solution (EBSS, Invitrogen) for 30 minutes at 37^{o}C in 5% CO_2. The cells were mechanically dissociated in the presence of DNaseI and seeded onto 13 mm poly-D-lysine-coated coverslips in a 50 μl droplet of Dulbecco's modified Eagle's medium (DMEM, Invitrogen) containing 0.5% FCS at a density of 2.5x10^{5} cells/coverslip. The cells were allowed to attach for 30 minutes. 350 μl of defined medium (Bottenstein and Sato, 1979) was added and incubation continued at 37^{o}C in 5% CO_2. Cyclopamine was used at a final concentration of 1 μM and the FGFR inhibitor PD173074 at 100 nM.

Results

Generation of Dbx1-iCre transgenic mice

To generate mice expressing Cre recombinase under (Sigma) and post-fixed PACce

small region of the neuroepithelium. From E16.5 onwards all transcript expression was abolished (data not shown). We selected one of these lines for further study.

To establish the dorsal and ventral limits of Cre expression in the neuroepithelium, we crossed the *Dbx1-Cre* mice to the *Rosa26-GFP* reporter line (Mao et al., 2001) and analyzed the offspring at embryonic day 10.5 (E10.5) by in situ hybridization. GFP expression was activated in a broad neuroepithelial domain, wider than the domain of *Dbx1* expression at the same age but corresponding more closely to *Dbx2* (Fig. 2A-C). This is consistent with previous reports that *Dbx1* is initially expressed (prior to E10.5) in an identical pattern to *Dbx2* and only narrows down later (Pierani et al., 2001). The region of GFP activation therefore probably corresponds to the early *Dbx1/ Dbx2* co-expression domain. The ventral limit of GFP expression abuts the dorsal limit of *Nkx6.1*, many cell diameters away from the *Olig2*-expressing domain in pMN (Fig. 2D-F). This is consistent with previous data showing mutually exclusive expression of Nkx6.1 and Dbx2 in the spinal cord (Briscoe et al., 2000). The dorsal limit of GFP activation overlaps with Mash1 and Pax7 which are expressed within dP5 or dP6, respectively, at their ventral limit (Fig. 2G-I) (Caspary and Anderson, 2003; Helms and Johnson, 2003). Collectively, the data demonstrate that expression of iCre is restricted to *Dbx1/Dbx2*-positive neuroepithelial precursors and activation of the GFP reporter gene is therefore restricted to four domains of the neuroepithelium: dP5, dP6, P0 and P1 (Fig. 1E).

We examined the distribution of GFP in *Dbx1-iCre x Rosa26-GFP* embryos around the time of neurogenesis in the spinal cord (E12.5). At E12.5, GFP-labelled cells were found exclusively in the ventral and lateral spinal cord (Fig. 3A). GFP-labelled axons were observed in the developing ventral white matter, including commissural axon tracts (Fig. 3A). Subsets of GFP-labelled neurons in the lateral cord co-expressed Lbx1, which marks early postmitotic neurons derived from dP4, dP5 and dP6 (Muller et al., 2002) (Fig. 3D). Other GFP-labelled neurons in the ventral spinal cord expressed Evx1, which marks neurons derived from the p0 domain (Moran-Rivard et al., 2001) (Fig. 3E) and En1, which marks V1 interneurons in the lateral cord (not shown) (Saueressig et al., 1999). The majority of the GFP-labelled cells observed in the spinal cord at this stage co-expressed the homeodomain transcription factor Lim2 (Fig. 3F), which is expressed in a variety of postmitotic neurons (Tsuchida et al., 1994).

In contrast, there was no co-expression of GFP in Isl1/ Isl2-positive neurons derived from pMN or dP3 (Fig. 3B) (Tsuchida et al., 1994) or in Lim3-positive interneurons derived from p2 or motor neurons from pMN (Fig. 3C) (Tsuchida et al., 1994). In conclusion, and as

processes, typical of maturing oligodendrocytes. They comprised around 3% of the total

of fine branched processes labelled with GFP Fig. 8C-F). Some protoplasmic astrocytes co-labelled weakly with anti-GFAP (Fig. 8D) and all expressed S100β (Fig. 8C). They were interspersed among dorsal neurons (not shown) and motor neurons (Fig. 8E). They also formed bilateral, longitudinal columns of cells positioned adjacent to the central canal

There have been previous suggestions of a dorsal source(s) of oligodendrocytes in the rodent cervical spinal cord and hindbrain, based on early expression of the myelin proteolipid

correspond to the neuroepithelial precursors themselves (Malatesta et al., 2003; Anthony et al., 2004). From E15.5, when the radial glial cell bodies moved towards the pial surface, we observed co-expression of RC2 and the oligodendrocyte lineage markers Olig2 or Sox10 in some radially-oriented cells, suggesting that the radial glia transform directly into oligodendrocytes. This supports previous evidence that spinal cord radial glia can give rise to oligodendrocytes as well as astrocytes after neuron generation has ceased (Choi et al., 1983; Choi and Kim, 1985; Hirano and Goldman, 1988).

It is not clear whether the mode of OLP generation from *Dbx* expressing precursors is fundamentally different from their mode of generation in the ventral cord. pMN-derived OLPs are presumably derived from radial glia too, since the latter are now thought to correspond to stem cells that generate all the neurons and glia of the CNS. However, the pMN-derived OLPs arise close to the ventricular surface whereas we first detected *Dbx*-derived OLPs towards the pial surface. This presumably relates to the position of the radial glial cell bodies at the time they start to express oligodendrocyte lineage markers such as Pdgfra, Sox10 or Olig2. Another difference seems to lie in how widely the OLPs disseminate after they are formed; those formed early from pMN proliferate rapidly at first and migrate away from pMN in all directions whereas the later-forming Dbx-derived OLPs proliferate less strongly, if at all, and migrate less widely. It remains to be determined whether these different behaviours reflect different inducing signals (Shh versus FGF, say), different environments in the cord at early versus late embryonic stages, or some intrinsic difference between the ventral and dorsal subsets.

Two types of astrocytes are generated from the Dbx domain

In addition to interneurons and oligodendrocytes, at least two morphological subtypes of astrocytes were generated from the *Dbx* domain. Protoplasmic astrocytes had a typical spherical outline with an extensive and intricate network of sheet-like branching processes and were distributed widely within the gray matter of the spinal cord. They were frequently associated with the cell bodies of neurons in both the dorsal and ventral cord, including motor neurons. Fibrous astrocytes on the other hand had a restricted distribution within the lateral white matter - in those regions previously occupied by the distal ends of the radial glia processes. The latter observation is consistent with the idea that some radial glia transform directly into fibrous astrocytes at the end of neuronogenesis (Schmechel and Rakic, 1979; Voigt, 1989; see Goldman, 2001 for review).

Our *Dbx1-iCre* mice label the progeny of four neuroepithelial domains – p1, p0, dP6 and dP5 – so we cannot tell whether each one of these domains generates all of the glial cell types

described here or whether different subsets of glia are generated from each individual domain, as has been shown for neurons. Resolution of this question would require targeting of the Cre transgene to individual neuroepithelial domains within the broader Dbx domain - not possible with currently available Cre deleter strains.

Dbx-neuroepithelial cells do not generate ependymal cells

We observed that *Dbx1/ Dbx2* precursors do not contribute to the ependymal layer that surrounds the reduced lumen of the postnatal and adult spinal cord, adding to previous evidence that ependymal cells are derived entirely from ventral (Nkx6.1-expressing) neuroepithelium (Richardson et al., 1997; Fu et al., 2003). Nevertheless, a subset of the *Dbx*-derived protoplasmic astrocytes settles close to the postnatal ependymal layer where they form narrow bilateral columns of cells along the length of the spinal cord. It is interesting to speculate that these might correspond to a subset of "subependymal astrocytes" analogous to those that have been described as neural stem cells in the postnatal telencephalon (Doetsch et al., 1999).

Acknowledgements

We thank Matthew Grist for technical assistance, Ulla Dennehy and Palma Iannarelli for transgenic mouse production and our colleagues for useful discussions. We also thank Tom Jessell, David Rowitch, Michael Wegner, Rolf Sprengel and Neal Copeland for antibodies and plasmids, Jaime Carvajal for advice about PAC recombination and Nigel Pringle for help with immunohistochemistry. We thank Stephen Skaper for PD173074 and William Gaffield for cyclopamine. Work in the authors' laboratory is supported by the Wellcome Trust Functional Genomics Initiative, the UK Medical Research Council and a Wellcome Trust Studentship to Matthew Fogarty.

Note added in proof

While this article was being reviewed, two other articles were published that demonstrate production of a subset of oligodendrocyte precursors in the dorsal VZ (dP3, dP4 and dP5) [**Cai, J., Qi, Y., Hu, X., Tan, M., Liu, Z., Zhang, J., Li, Q., Sander, M., and Qiu, M.** (2005). Generation of oligodendrocyte precursor cells from mouse dorsal spinal cord independent of *Nkx6l*-regulation and *Shh* signalling. *Neuron* **45**, 41-53; **Vallstedt, A., Klos, J.M., and Ericson, J.** (2005). Multiple dorsoventral origins of oligodendrocyte generation in the spinal cord and hindbrain. *Neuron* **45**, 55-67; reviewed by **Miller, R.H.** (2005). Dorsally derived oligodendrocytes come of age. *Neuron* **45**, 1-3.]

References

Agius, E., Soukkarieh, C., Danesin, C., Kan, P., Takebayashi, H., Soula, C., and Cochard, P.

Doetsch, F., Caille, I., Lim, D. A., Garcia-Verdugo, J. M., and Alvarez-Buylla, A. (1999). Subventricular zone astrocytes are neural stem cells in the adult mammalian brain. *Cell* **97,** 703-716.

Fruttiger, M., Karlsson, L., Hall, A. C., Abramsson, A., Calver, A. R., Bostrom, H., Willetts, K., Bertold, C. H., Heath, J. K., Betsholtz, C., and Richardson, W.D. (1999). Defective oligodendrocyte development and severe hypomyelination in PDGF-A knockout mice. *Development* **126,** 457-467.

Fu, H., Qi, Y., Tan, M., Cai, J., Hu, X., Liu, Z., Jensen, J., and Qiu, M. (2003). Molecular mapping of the origin of postnatal spinal cord ependymal cells: evidence that adult ependymal cells are derived from Nkx6.1+ ventral neural progenitor cells. *J. Comp Neurol.* **456,** 237-244.

Goldman, J. E. (2001). Developmental origins of astrocytes. In *Glial cell development*. (ed. Jessen,K.R. and Richardson,W.D.), pp. 55-74. Oxford, New York: Oxford Univerity Press.

Helms, A. W. and Johnson, J. E. (2003). Specification of dorsal spinal cord interneurons. *Curr. Opin. Neurobiol.* **13,** 42-49.

Hirano, M. and Goldman, J. E. (1988). Gliogenesis in the rat spinal cord: Evidence for origin of astrocytes and oligodendrocytes from radial precursors. *J. Neurosci. Res.* **21,** 155-167.

Incardona, J.P., Gaffield, W., Kapur, R.P. and Roelink H. (1998). The teratogenic Veratrum alkaloid cyclopamine inhibits sonic hedgehog signal transduction. *Development* **125**, 3553-3562.

Kessaris, N., Jamen, F., Rubin, L. L., and Richardson, W. D. (2004). Cooperation between sonic hedgehog and fibroblast growth factor/MAPK signalling pathways in neocortical precursors. *Development* **131,** 1289-1298.

Lee, E. C., Yu, D., Martinez, D. V, Tessarollo, L., Swing, D. A., Court, D. L, Jenkins, N. A., and Copeland, N. G. (2001). A highly efficient Escherichia coli-based chromosome engineering system adapted for recombinogenic targeting and subcloning of BAC DNA. *Genomics* **73,** 56-65.

Lu, Q. R., Sun, T., Zhu, Z., Ma, N., Garcia, M., Stiles, C. D., and Rowitch, D. H. (2002). Common developmental requirement for Olig function indicates a motor neuron/ oligodendrocyte connection. *Cell* **109,** 75-86.

Pringle, N. P. and Richardson, W. D. (1993). A singularity of PDGF alpha-receptor expression in the dorsoventral axis of the neural tube may define the origin of the oligodendrocyte lineage. *Development* **117,** 525-533.

Pringle, N. P., Yu, W.-P., Guthrie, S., Roelink, H., Lumsden, A., Peterson, A. C., and Richardson, W. D. (1996). Determination of neuroepithelial cell fate: induction of the oligodendrocyte lineage by ventral midline cells and sonic hedgehog. *Dev. Biol.* **177,** 30-42.

Pringle, N. P., Guthrie, S., Lumsden, A., and Richardson, W. D. (1998). Dorsal spinal cord neuroepithelium generates astrocytes but not oligodendrocytes. *Neuron* **20,** 883-893.

Pringle, N. P., Yu, W.-P., Howell, M., Colvin, J. S., Ornitz, D. M., and Richardson, W. D. (2003). Fgfr3 expression by astrocytes and their precursors: evidence that astrocytes and oligodendrocytes originate in distinct neuroepithelial domains. *Development* **130,** 93-102.

Richardson, W. D., Pringle, N. P., Yu, W.-P., and Hall, A. C. (1997). Origins of spinal cord oligodendrocytes: possible developmental and evolutionary relationships with motor neurons. *Dev. Neurosci.* **19,** 58-68.

Richardson, W. D., Smith, H. K., Sun, T., Pringle, N. P., Hall, A., and Woodruff, R. (2000). Oligodendrocyte lineage and the motor neuron connection. *Glia* **29,** 136-142.

Rowitch, D. H. (2004). Glial specification in the vertebrate neural tube. *Nat. Rev. Neurosci.* **5**, 409-419.

Saueressig, H., Burrill, J., and Goulding, M. (1999). Engrailed-1 and netrin-1 regulate axon pathfinding by association interneurons that project to motor neurons. *Development* **126,** 4201-4212.

Schmechel, D. E. and Rakic, P. (1979). A Golgi study of radial glial cells in developing monkey telencephalon: morphogenesis and transformation into astrocytes. *Anat. Embryol. (Berl)* **156,** 115-152.

Shimshek, D. R., Kim, J., Hubner, M. R., Spergel, D. J., Buchholz, F., Casanova, E., Stewart, A. F., Seeburg, P. H., and Sprengel, R. (2002). Codon-improved Cre recombinase (iCre) expression in the mouse. 193-

Figure Legends

Figure 1 Generation of *Dbx1-iCre* PAC transgenic mice and expression of the transgene. (A) Map of PAC 631-M19 indicating the extent of upstream and downstream genomic regions in the PAC insert. (B) Schematic of the endogenous Dbx1 locus including intron - exon structure and relative locations of *Bgl*II and *Hind*III restriction sites. (C) The targeting vector used in homologous recombination indicating the positions of the iCre coding sequences, chloramphenicol resistance cassette (*Cm*^{r}), loxP sites and the location of the 0.5 kb 3' UTR probe used to hybridize to Southern blots of *Bgl*II – digested genomic DNA. The locations of PCR primers used for genotyping are also indicated. (D) Expression of the iCre transgene at E11.5, revealed by in situ hybridization. Four independent founders had the same pattern of expression at this age. One founder was chosen for further study. (E) Diagram of neuroepithelial precursor domains in the spinal cord, and the reported patterns of

Figure 5 Oligodendrocytes are generated from *Dbx*-derived radial glia. Radially orientated GFP-positive cells express the oligodendrocyte lineage markers Olig2 (A, C) and Sox10 (B, D) at E16.5 (A-B) and E18.5 (C-D). Co-localization of the radial glia marker RC2 with GFP-labelled Olig2-positive cells at E15.5 (E, F, G, H) and E16.5 (I, J, K, L) or GFP-labelled Sox10-positive cells at E16.5 (M, N, O, P). Scale bar: 50 μm.

Figure 6 *Dbx*-derived oligodendrocytes at P10. (A) GFP and Sox10 double-immunolabelling. (B) Higher magnification confocal view of the area marked in (A), showing clear co-expression in a subset of Sox10-positive oligodendrocyte lineage cells. (C) GFP and PDGFRa double immuno-labelling. (D) double immuno-labelling of GFP and the differentiated oligodendrocyte marker CC1 (Bhat et al., 1996). Scale bar: 300 μm.

Figure 7 Shh-independent oligodendrocyte development from *Dbx*-derived precursors. Dissociated spinal cords from *Dbx1-iCre x Rosa26-GFP* embryos developed Sox10-positive OLPs within 5 days of culture (A). Their development was not inhibited by cyclopamine (B) but was abolished in the Tc57Tce of PD173074 (C) or both (D). (E) The experiment was quantified by counting the total number of double-labelled GFP-positive / Sox10-positive cells in the cultures. A minimum of 1000 Sox10-positive cells was counted for each condition. Similar data were obtained in two independent experiments.

Figure 8 Fibrous and protoplasmic astrocytes are derived from the *Dbx* expressing neuroepithelium. (A-B) Co-localization between GFAP (red) and GFP (green) in fibrous astrocytes in the developing white matter of a P10 spinal cord. (B) Confocal microscope view of the area highlighted in (A). (C-F) Protoplasmic astrocytes develop from *Dbx* precursors. (C) All GFP-positive protoplasmic astrocytes co-label with anti-S100β. (D) Protoplasmic astrocytes next to the central canal weakly co-expressed GFAP (arrows). (E-F) GFP (green) and NeuN (red) double labelling in (E) the ventral horn, lying in close proximity to motor neuron cell bodies. (F) Protoplasmic-like astrocytes form bilateral longitudinal columns of cells positioned adjacent to the central canal. Scale bars: (A) 200 μm, (C) 20 μm.

Figure 9 The origins of oligodendrocytes in the embryonic rodent spinal cord. From E12.5 in the mouse, OLPs are generated from pMN in the ventral VZ. Later, from approximately E16, a subsidiary population emerges from radial glial cells in the Dbx1-expressing domain that spans the dorsal-ventral midline. The latter population contributes around 5% of all oligodendrocyte lineage cells in the postnatal cord. Our data do not rule out the possibility that there are additional minor sources of oligodendrocytes outside either pMN or the Dbx domain.

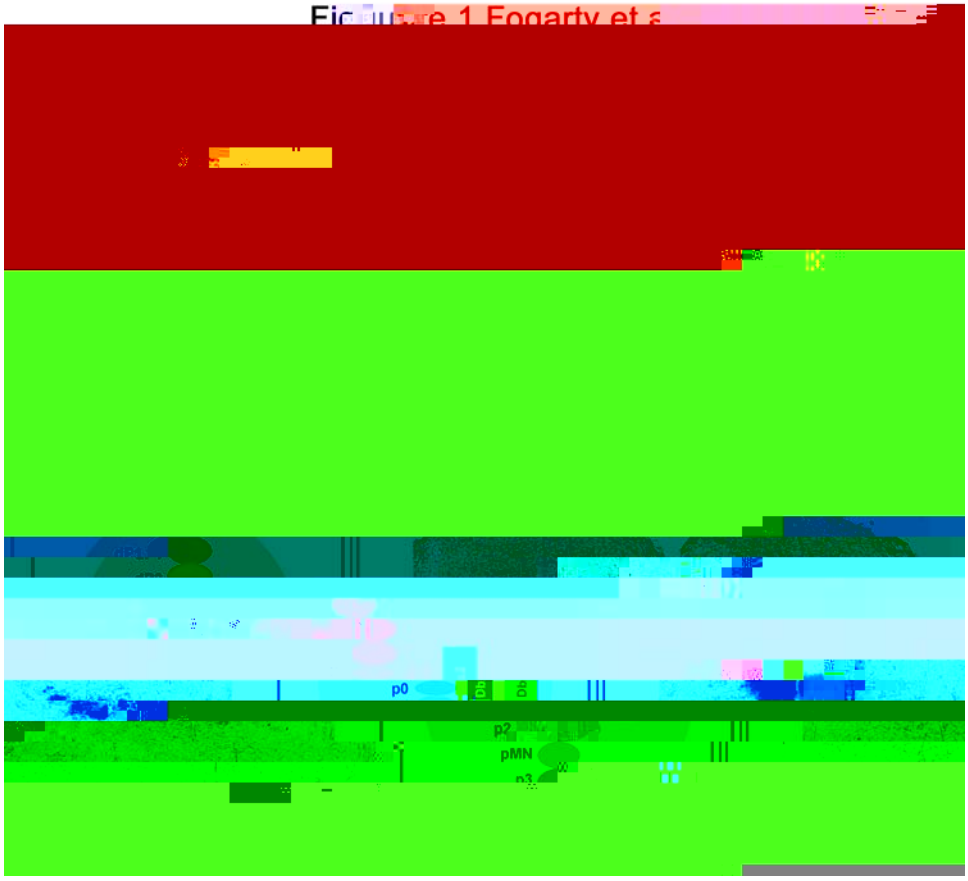
p0
p2
pMN
p3

Figure 2 Fogarty et al

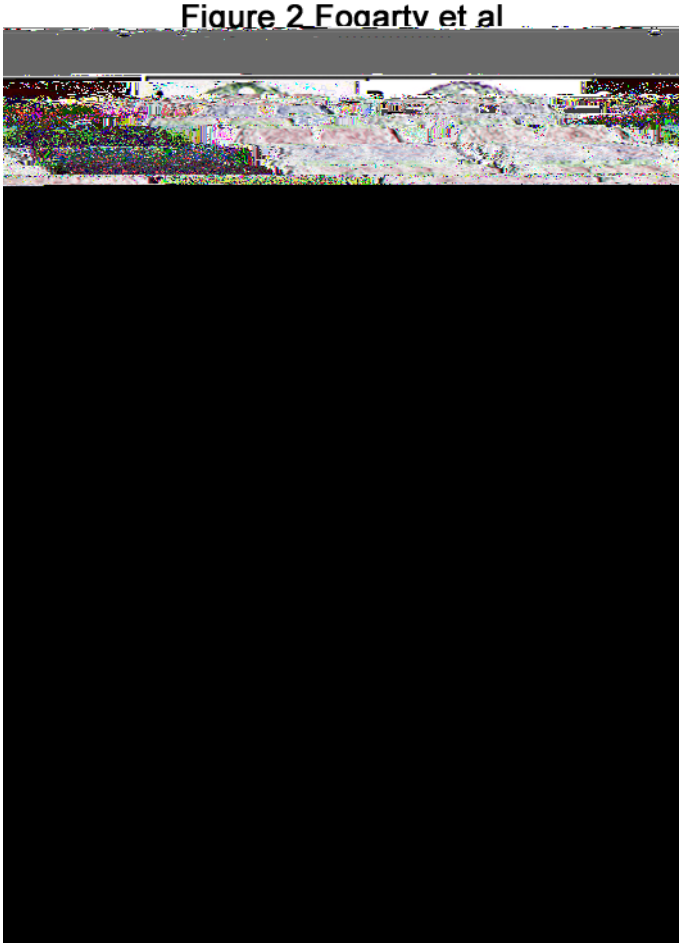

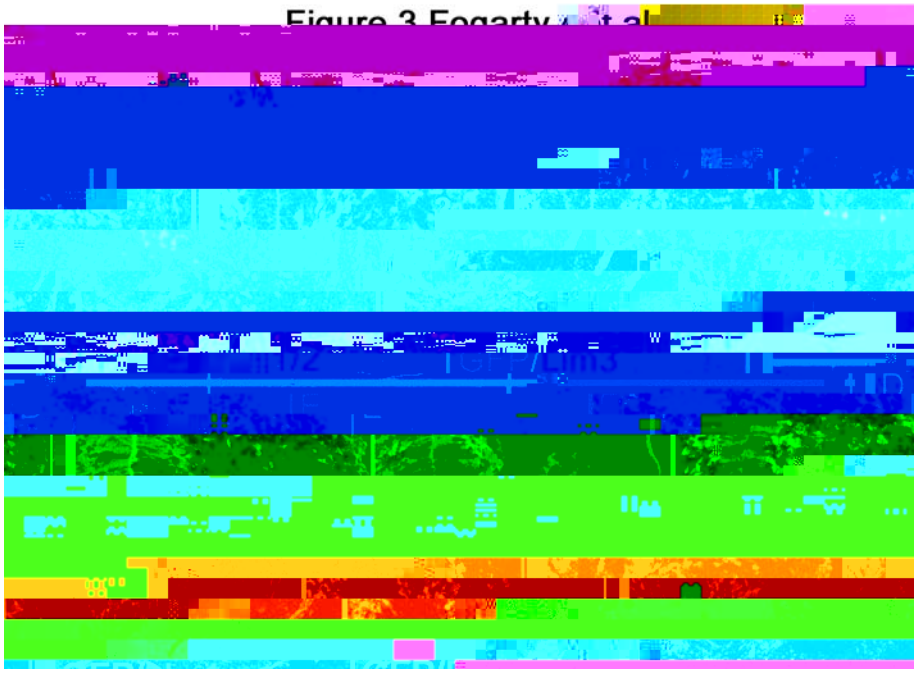

Figure 4 Fogart et al

Figure 6 Fogarty et al

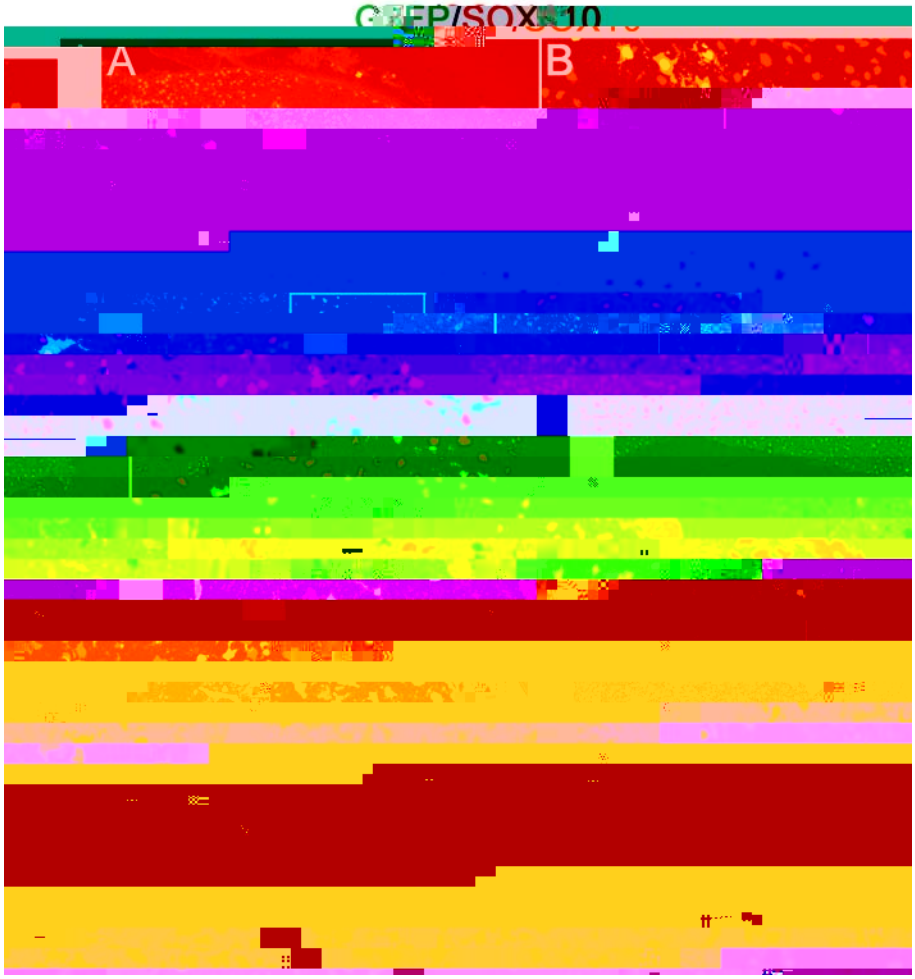

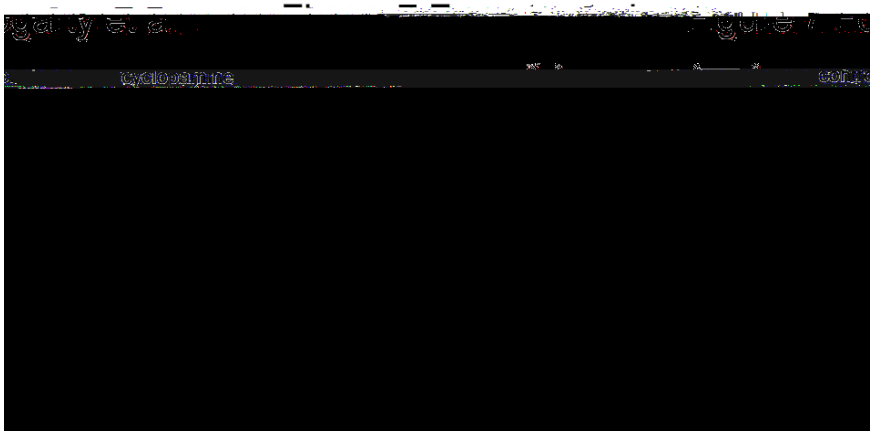

Figure 8 Fogarty et al